

AD-A166 685

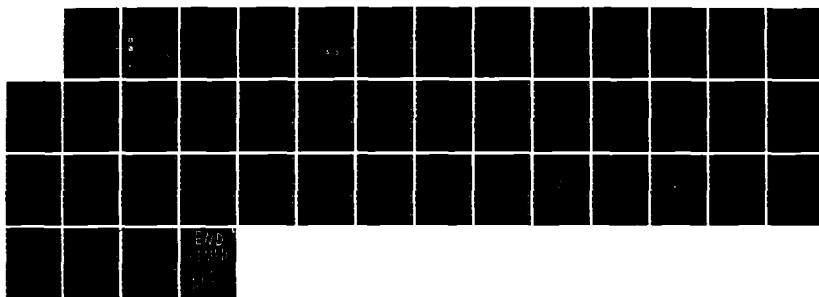
SHUTTLE CONTAMINATION MODELING: THE PLASMA WAVE FIELD
OF SPACECRAFT(U) AIR FORCE GEOPHYSICS LAB HANSCOM AFB
MA H HEINEMANN 22 NOV 85 AFGL-TR-85-0300

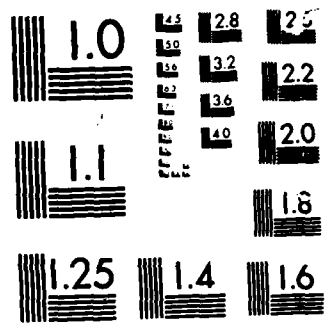
1/1

UNCLASSIFIED

F/G 22/1

NL





MICROCOPY

CHART

AD-A166 605

AFGL-TR-85-0300

ENVIRONMENTAL RESEARCH PAPERS, NO. 936

Shuttle Contamination Modeling: The Plasma Wave Field of Spacecraft

MICHAEL HEINEMANN



22 November 1985



Approved for public release; distribution unlimited.



DTIC FILE COPY



SPACE PHYSICS DIVISION

PROJECT 7661


AIR FORCE GEOPHYSICS LABORATORY

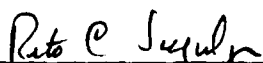
HANSCOM AFB, MA 01731

DTIC
ELECTE
APR 15 1986
S B D

"This technical report has been reviewed and is approved for publication"

FOR THE COMMANDER


CHARLES P. PIKE, Chief
Spacecraft Interactions Branch


RITA C. SAGALYN, Director
Space Physics Division

This document has been reviewed by the ESD Public Affairs Office (PA) and is releasable to the National Technical Information Service (NTIS).

Qualified requestors may obtain additional copies from the Defense Technical Information Center. All others should apply to the National Technical Information Service.

If your address has changed, or if you wish to be removed from the mailing list, or if the addressee is no longer employed by your organization, please notify AFGL/DAA, Hanscom AFB, MA 01731. This will assist us in maintaining a current mailing list.

Unclassified

ADA 166605

SECURITY CLASSIFICATION OF THIS PAGE

REPORT DOCUMENTATION PAGE				
1a. REPORT SECURITY CLASSIFICATION Unclassified			1b. RESTRICTIVE MARKINGS	
2a. SECURITY CLASSIFICATION AUTHORITY			3. DISTRIBUTION/AVAILABILITY OF REPORT	
2b. DECLASSIFICATION/DOWNGRADING SCHEDULE			Approved for public release; distribution unlimited	
4. PERFORMING ORGANIZATION REPORT NUMBER(S) AFGL-TR-85-0300 ERP No. 936			5. MONITORING ORGANIZATION REPORT NUMBER(S)	
6a. NAME OF PERFORMING ORGANIZATION Air Force Geophysics Laboratory		6b. OFFICE SYMBOL (If applicable) PHK	7a. NAME OF MONITORING ORGANIZATION	
6c. ADDRESS (City, State and ZIP Code) Hanscom AFB Massachusetts 01731		7b. ADDRESS (City, State and ZIP Code)		
8a. NAME OF FUNDING/SPONSORING ORGANIZATION		8b. OFFICE SYMBOL (If applicable)	9. PROCUREMENT INSTRUMENT IDENTIFICATION NUMBER	
8c. ADDRESS (City, State and ZIP Code)		10. SOURCE OF FUNDING NOS.		
		PROGRAM ELEMENT NO.	PROJECT NO.	TASK NO.
		62101F	7661	11
11. TITLE (Include Security Classification) Shuttle Contamination Modeling: The Plasma (cont.)		WORK UNIT NO. 02		
12. PERSONAL AUTHOR(S) Michael Heinemann				
13a. TYPE OF REPORT Scientific Interim		13b. TIME COVERED FROM TO	14. DATE OF REPORT (Yr., Mo., Day) 1985 November 22	15. PAGE COUNT 42
16. SUPPLEMENTARY NOTATION				
17. COSATI CODES			18. SUBJECT TERMS (Continue on reverse if necessary and identify by block number)	
FIELD	GROUP	SUB GR	Shock waves Alfven waves Whistler waves	
			Upper hybrid waves Plasma waves	
19. ABSTRACT (Continue on reverse if necessary and identify by block number) We investigate the behavior of waves and shock-like disturbances produced by the interaction of spacecraft with the plasma environment. We find that (1) there are three ranges of wave frequency for which waves can propagate to large distances from the spacecraft, (2) that waves in these frequency ranges are confined to propagate within specific ranges of directions, and (3) that it is possible for these waves to form shocks. Approximate analytic solutions are given to describe the behavior of waves and shocks of spacecraft origin. The waves that are important to these phenomena can be classed as Alfven, whistler, and upper hybrid waves. While we believe it unlikely to occur, we have identified analytically those conditions necessary for extremely rapid spatial wave growth near the spacecraft.				
20. DISTRIBUTION/AVAILABILITY OF ABSTRACT UNCLASSIFIED/UNLIMITED <input checked="" type="checkbox"/> SAME AS RPT <input type="checkbox"/> DTIC USERS <input type="checkbox"/>			21. ABSTRACT SECURITY CLASSIFICATION Unclassified	
22a. NAME OF RESPONSIBLE INDIVIDUAL Michael Heinemann			22b. TELEPHONE NUMBER (Include Area Code) 617-861-3240	22c. OFFICE SYMBOL PHK

DD FORM 1473, 83 APR

EDITION OF 1 JAN 73 IS OBSOLETE

SECURITY CLASSIFICATION OF THIS PAGE

Unclassified

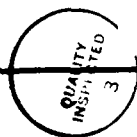
SECURITY CLASSIFICATION OF THIS PAGE

Block 11 (cont.)

Wave Field of Spacecraft

Accession For	
NTIS GRA&I	<input checked="checked" type="checkbox"/>
DTIC TAB	<input type="checkbox"/>
Unannounced	<input type="checkbox"/>
Justification	
By	
Distribution/	
Availability Codes	
Dist	Avail and/or Special
A-1	

DTIC
ELECTE
APR 15 1986
S B



Unclassified

SECURITY CLASSIFICATION OF THIS PAGE

Contents

1. INTRODUCTION	1
2. COLD PLASMA WAVES	4
3. THE CHARACTERISTICS GOVERNING WAVE PROPAGATION	8
3.1 Propagation of Discontinuities	12
3.2 Phase and Group Velocities	13
4. PROGRESSING WAVE SOLUTIONS	18
5. STEADY PLASMA STRUCTURE AROUND A MOVING SOURCE	25
6. APPLICATIONS TO SPACECRAFT	28
7. DISCUSSION	33
REFERENCES	35
APPENDIX	37

Illustrations

1. The Angle Between the Characteristics and the Magnetic Field, Given as a Function of Wave Frequency, for a Hydrogen Plasma With $n = 10^4 \text{ cm}^{-3}$ and $B = 0.3 \text{ G}$	11
2. The Phase and Group Velocities of Low Frequency Plasma Waves, Given as Functions of Angle With Respect to the Magnetic Field	18

Illustrations

3. The Parameter ϵ_* Plotted as a Function of Wave Frequency	24
4. Construction of the Characteristics for a Moving Source	30
5. Qualitative View of the Three-Dimensional Limits of the Wave Field for a Given Frequency and $\epsilon_* < 0$	32
6. Qualitative View of the Three-Dimensional Limits of the Wave Field for a Given Frequency and $\epsilon_* > 0$	33

Tables

1. Frequencies for Which There Are Real Characteristics	10
---	----

Shuttle Contamination Modeling: The Plasma Wave Field of Spacecraft

1. INTRODUCTION

Shuttle and other low altitude Earth orbit spacecraft move through a medium that is characterized by a neutral number density of about 10^9 cm^{-3} and an ion density of $10^4 - 10^5 \text{ cm}^{-3}$. Typical collisional mean-free paths are on the order of kilometers or greater, precluding a strong collisional interaction with the spacecraft which would produce collision-dominated waves and shocks. The long mean-free paths also mean that the interaction between the ambient ions and neutrals is weak on the scale of kilometers, so that the ions may be treated as a collisionless plasma on this scale. Typical temperatures at shuttle altitude are on the order of 1000 K, so that the electron thermal speed is on the order of 100 km/sec, about an order of magnitude less than the Alfvén speed. As a result, the plasma may be treated in the cold plasma approximation. A spacecraft moving through such a cold, collisionless plasma can be expected to produce waves and shocks or shock like structures.

Typical phase and group velocities of cold plasma waves are on the order of the Alfvén speed. As such, shock waves could be regarded as unlikely, because the spacecraft velocity is a few kilometers per second, quite small compared to

(Received for publication 13 November 1985)

the wave speeds. However, cold plasma waves range from almost isotropic to quite anisotropic. For some wave modes, the phase or group velocity goes to zero in certain directions with respect to the background geomagnetic field.^{1,2} The possibility exists that these modes can be shocked by any spacecraft velocity, no matter how small.

The interaction between spacecraft and the ambient plasma has been investigated by Drell et al³ and by Barnett and Olbert.⁴ Drell et al showed that spacecraft could produce Alfvén wings, a steady Alfvén disturbance extending away from the spacecraft. Barnett and Olbert have recently extended the analysis to include all plasma waves, although a written report is not yet available.

The purpose of the present paper is to describe the wave and shock structure of a spacecraft moving through a collisionless cold plasma. The focus of the work will be the spatial properties of those waves, produced by the interaction of the spacecraft with the ambient plasma, which can propagate to great distances from the spacecraft and can form shock-like disturbances. These waves, unlike waves which propagate isotropically, can propagate only within sharply defined spatial regions. Our methods lead to definite predictions for (1) the frequencies of waves which can propagate to large distances from the spacecraft, (2) the directions within which they can propagate, (3) the wave power spectrum around the spacecraft, and (4) predictions of shock-like disturbances.

An important restriction of our results should be mentioned here. We use essentially two-dimensional methods throughout. The formalism involved in the three-dimensional problem is sufficiently complicated that, without the two-dimensional formulation as introduction, the results are essentially unreadable. Qualitatively, a two-dimensional treatment is no great impediment. The typical properties, exemplified by the characteristics, are similar in three dimensions. However, the quantitative details should be regarded and used with a certain amount of discretion; the details can be expected to change in three dimensions.

One motive for this work is to begin a fundamental investigation of the interaction of spacecraft with the plasma environment. Such an investigation is necessary to treat a wide range of issues, some of traditional importance, some newly

-
1. Stix, T.H. (1962) The Theory of Plasma Waves, McGraw-Hill, New York.
 2. Musielak, Z.E. (1984) M.I.T. Center for Space Research Report No. CSR-TR-84-3.
 3. Drell, S.D., Foley, H.M., and Ruderman, M.A. (1965) Drag and propulsion of large satellites in the ionosphere: An Alfvén propulsion engine in space, J. Geophys. Res. 70:3131.
 4. Barnett, A., and Olbert, S. (1985) Radiation of plasma waves by a conducting body moving through a magnetized plasma, submitted to J. Geophys. Res.

emerging. These issues can be broadly classed under two main headings: spacecraft charging and spacecraft contamination.

Spacecraft charging issues include charging of the spacecraft itself, wake formation, and density enhancements in ram. These are all affected, at least in principle, by plasma waves and turbulence. A particularly pressing issue is the interaction of the wake with waves and turbulence and the consequent effect on charging.

Spacecraft contamination issues include spacecraft glow, ionization of high density contaminants of spacecraft origin, and, possibly, extended plasma radiation processes. While the present work cannot hope to address all of these topics, it should at least provide the basis for addressing several of them, including effects of waves on charging and the evolution of plasma clouds.

A second motive for this work is to provide the mathematical and physical basis for modeling of the spacecraft interaction. Current efforts are largely limited to purely numerical work (for example, the NASCAP and POLAR codes) because of the intractability of the physics as well as the complications arising from the geometry of real spacecraft. These codes are typically unwieldy and limited by the simplifying assumptions necessary to produce a computer program that runs in a finite length of time. If one contemplates, as we do, computer modeling of a wide range of spacecraft interactions, including charging, contamination, surface chemistry, chemical reactions, molecular transport, ionization processes, and the formation of plasma waves and turbulence, while perhaps including the effects of charged particle beams, the probability of success with a purely numerical approach appears to be negligible; the reason one cannot see the light at the end of the tunnel is because there is no end to the tunnel. The approach that we advocate, and that has had reasonable success in the development of the NASCAP and POLAR codes, is to reduce each part of the problem to manageable proportions using analytical techniques where possible. This paper, we hope, represents a contribution to that process.

In the following sections, we will treat cold plasma waves in a homogeneous medium directly from the point of view of the governing differential equations. From the equations, we will determine the characteristics that govern wave propagation and show that there are three different frequency domains in which waves can propagate to large distances from the spacecraft. The propagation of discontinuities is discussed in terms of and related to the characteristics. The relation between cold plasma resonances and the characteristics of the differential equations is pointed out, and a physical picture of the characteristics as carriers of discontinuities is developed from the plane wave picture. Solutions of the cold plasma equations appropriate for localized disturbances are then determined ana-

lytically; they provide a prediction of the power spectrum of fluctuations far from the spacecraft. Finally, applications to the spacecraft environment are discussed.

2. COLD PLASMA WAVES

The treatment of plasma waves begins with a standard approach to the problem. We include it to establish approach and notation. The aim is to write partial differential equations governing waves in a cold plasma. In particular, we shall reduce the problem to a fourth order partial differential equation for a magnetic field fluctuation.

The linearized cold plasma equation of motion is

$$(\partial/\partial t)\delta\vec{V}_\alpha = (e_\alpha/m_\alpha)\delta\vec{E} + (e_\alpha/m_\alpha c)\delta\vec{V}_\alpha \times \vec{B} \quad (1)$$

where α indicates the species of particle, e_α is its charge, m_α its mass, $\delta\vec{V}_\alpha$ is the bulk velocity of the species, $\delta\vec{E}$ is the electric field, δ indicates fluctuating quantities, and c is the speed of light. The solution for $\delta\vec{V}$ with a harmonic time dependence, $\partial/\partial t = -i\omega$, is

$$\delta V_\parallel = (e_\alpha/m_\alpha)(i\omega/\omega^2) \delta E \quad (2)$$

$$\delta\vec{V}_\perp = (e_\alpha/m_\alpha)(i\omega\delta\vec{E}_\perp + \delta\vec{E} \times \vec{Q}_\alpha) / (\omega^2 - \Omega_\alpha^2) \quad (3)$$

where \parallel and \perp mean parallel and perpendicular to the background magnetic field, and the gyrofrequency of species α is defined by

$$\vec{Q}_\alpha = -e_\alpha\vec{B}/(m_\alpha c). \quad (4)$$

We note that the frequency ω is defined in the proper frame of the plasma (the frame in which the background plasma is at rest) and that the frequency measured by an observer moving through the plasma with a velocity \vec{U} is $\omega' = \omega + \vec{k} \cdot \vec{U}$, where \vec{k} is the wave vector.

The current density, defined by

$$\delta\vec{J} = \sum_\alpha n_\alpha e_\alpha \delta\vec{V} \quad (5)$$

where n_α is the number density of species α , is

$$\begin{aligned} \delta \vec{J} = & (i\omega/4\pi)(\omega_p^2/\omega^2) \delta \vec{E}_{\parallel} + (i\omega/4\pi) \sum_{\alpha} [\omega_{p\alpha}^2/(\omega^2 - \Omega_{\alpha}^2)] \delta \vec{E}_{\perp} \\ & + (1/4\pi) [\sum_{\alpha} \omega_{p\alpha}^2 \Omega_{\alpha}/(\omega^2 - \Omega_{\alpha}^2)] \hat{b} \times \delta \vec{E} \end{aligned} \quad (6)$$

where

$$\omega_{p\alpha}^2 = 4\pi n_{\alpha} e_{\alpha}^2 / m_{\alpha} \quad (7)$$

is the plasma frequency of species α , the plasma frequency is

$$\omega_p^2 = \sum_{\alpha} \omega_{p\alpha}^2 \quad (8)$$

and $\hat{b} = \vec{B}/B$ is a unit vector in the direction of the field. Inserting Eq. (6) into the combined Ampere-Faraday Law

$$\vec{\nabla} \times (\vec{\nabla} \times \delta \vec{E}) = (4\pi i\omega/c^2) \delta \vec{J} + (\omega^2/c^2) \delta \vec{E} \quad (9)$$

we obtain

$$\vec{\nabla} \times (\vec{\nabla} \times \delta \vec{E}) = \epsilon_0 \delta \vec{E}_{\parallel} - \epsilon_P \delta \vec{E}_{\perp} - \epsilon_H \hat{b} \times \delta \vec{E} \quad (10)$$

where

$$\epsilon_0 = (\omega^2 - \omega_p^2)/c^2 \quad (11)$$

$$\epsilon_P = -(\omega^2/c^2) [1 - \sum_{\alpha} \omega_{p\alpha}^2/(\omega^2 - \Omega_{\alpha}^2)] \quad (12)$$

$$\epsilon_H = -(i\omega/c^2) \sum_{\alpha} \omega_{p\alpha}^2 \Omega_{\alpha}/(\omega^2 - \Omega_{\alpha}^2). \quad (13)$$

Our approach will be to write the differential equations in a homogeneous background plasma. To do this, we assume that the magnetic field is

$$\vec{B} = (0, 0, B_z) \quad (14)$$

and

$$\partial/\partial y \equiv 0$$

(15)

and that the coefficients ϵ are constant. Eq. (15) limits the subsequent analysis to two dimensions; this approach sacrifices generality for the sake of clarity. The assumption of constant magnetic field is consistent with the nature of the spacecraft interaction; the spacecraft is a small object in a large scale (on the order of one Earth radius) magnetic field. The assumption of constant ϵ , which implies that the number density is constant, is not very good; the density changes by orders of magnitude in a large region occupied by the spacecraft wake and perhaps in a smaller region in ram. As a result, the detailed results of wave propagation will be limited to a region outside the strong density gradients near the spacecraft. It is not difficult to generalize our differential equations to variable density, but the possibility of solving the equations analytically appears to be remote. With these assumptions, Eq. (10) becomes

$$-\partial_z(\partial_z \delta E_x - \partial_x \delta E_z) = -\epsilon_P \delta E_x + \epsilon_H \delta E_y \quad (16)$$

$$-(\partial_x^2 + \partial_z^2) \delta E_y = -\epsilon_H \delta E_x - \epsilon_P \delta E_y \quad (17)$$

$$\partial_x(\partial_z \delta E_x - \partial_x \delta E_z) = \epsilon_0 \delta E_z \quad (18)$$

where ∂_i means $\partial/\partial x_i$. Using the Faraday relation

$$\partial_t \delta B_y = -i\omega \delta B_y = -c(\partial_z \delta E_x - \partial_x \delta E_z) \quad (19)$$

where ∂_t means $\partial/\partial t$, Eqs. (16) through (18) can be written

$$(i\omega/c)\partial_z \delta B_y = \epsilon_P \delta E_x - \epsilon_H \delta E_y \quad (20)$$

$$(\partial_x^2 + \partial_z^2 - \epsilon_P) \delta E_y = \epsilon_H \delta E_x \quad (21)$$

$$(i\omega/c)\partial_x \delta B_y = \epsilon_0 \delta E_z \quad (22)$$

Eqs. (20) and (22) can be combined to yield

$$[\partial_z^2 - (\epsilon_P - \epsilon_0)\partial_x^2 - \epsilon_P] \delta B_y = -(c/i\omega) \epsilon_H \partial_z \delta E_y \quad (23)$$

or, because

$$(c/i\omega)\partial_z \delta E_y = -\delta B_x, \quad (24)$$

$$[\partial_z^2 - (\epsilon_P/\epsilon_0)\partial_x^2 - \epsilon_P] \delta B_y = \epsilon_H \delta B_x. \quad (25)$$

Similarly, Eq. (21) can be written (after differentiation with respect to z)

$$(\partial_x^2 + \partial_z^2 - \epsilon_P) \delta B_x = -\epsilon_H(1 + \epsilon_0^{-1}\partial_x^2) \delta B_y \quad (26)$$

where Faraday's Law has been used to eliminate derivatives of $\delta \vec{E}$.

For future reference, we should like to state that Eqs. (25) and (26) can be rewritten in the form

$$[\partial_z^2 - (\epsilon_P/\epsilon_0)\partial_x^2 - \epsilon_P] \alpha = \epsilon_H(1 + \epsilon_0^{-1}\partial_x^2) \beta \quad (27)$$

$$(\partial_x^2 + \partial_z^2 - \epsilon_P) \beta = -\epsilon_H \alpha \quad (28)$$

where α and β are defined by

$$\alpha = (1 + \epsilon_P/\epsilon_0) \delta B_y - (\epsilon_H/\epsilon_0) \delta B_x \quad (29)$$

$$\beta = (1 + \epsilon_P/\epsilon_0) \delta B_x + (\epsilon_H/\epsilon_0) \delta B_y. \quad (30)$$

Eqs. (25) and (26) or Eqs. (27) and (28) are a pair of coupled second order partial differential equations that govern linear waves in cold quasineutral plasmas. It is instructive to consider the low frequency limit of these equations. In the limit that $\omega \rightarrow 0$, it is easy to see that

$$\epsilon_P = -(\omega^2/c^2)(1 + c^2/V_A^2) \quad (31)$$

where

$$V_A = B/\sqrt{4\pi\rho} \quad (32)$$

is the nonrelativistic Alfvén speed, and

$$\epsilon_H = (4\pi i \omega / cB) \sum_{\alpha} n_{\alpha} e_{\alpha} = 0 \quad (33)$$

because of the quasineutrality of the background plasma, which we here assume. In this case, Eqs. (25) and (26) uncouple, and can be written

$$[\partial_z^2 - (\epsilon_P / \epsilon_0) \partial_x^2 - \epsilon_P] \delta B_y = 0 \quad (34)$$

$$(\partial_x^2 + \partial_z^2 - \epsilon_P) \delta B_x = 0. \quad (35)$$

These can be recognized as the Alfvén mode and fast mode, respectively. The Alfvén mode propagates approximately along the field, while the fast mode propagates isotropically.

Eqs. (25) and (26) can be reduced to a single equation:

$$\begin{aligned} & (\partial_x^2 + \partial_z^2 - \epsilon_P) [\partial_z^2 - (\epsilon_P / \epsilon_0) \partial_x^2 - \epsilon_P] \delta B_y \\ & + \epsilon_H^2 (1 + \epsilon_0^{-1} \partial_x^2) \delta B_y = 0 \end{aligned} \quad (36)$$

Eq. (36) is a single fourth order equation governing cold plasma waves.

3. THE CHARACTERISTICS GOVERNING WAVE PROPAGATION

By a standard mathematical procedure, the characteristics of the differential Eq. (36) can be determined by solving a first order partial differential equation

$$Q(\vec{\nabla} \phi) = 0 \quad (37)$$

(cf. Courant and Hilbert, 632⁵).

5. Courant, R., and Hilbert, D. (1962) Methods of Mathematical Physics (Vol. II), Interscience, New York.

In the case of Eq. (36), the characteristic equation is

$$(\phi_x^2 + \phi_z^2)[\phi_z^2 - (\epsilon_P/\epsilon_0)\phi_x^2] = 0. \quad (38)$$

There are two solutions for characteristic surfaces:

$$\phi_x^2 + \phi_z^2 = 0 \quad (39)$$

and

$$\phi_x^2 = (\epsilon_0/\epsilon_P)\phi_z^2. \quad (40)$$

Eq. (39) yields only imaginary surfaces. In the terminology of partial differential equations, it means that the problem is elliptic. Physically, it means that the waves associated with these characteristics propagate more or less isotropically. An example of completely isotropic propagation is the fast mode wave, described by Eq. (35). Because of the isotropic propagation, the wave amplitudes can be expected to fall off rapidly from a confined source. The falloff for fast mode waves is $1/r^2$. While the falloff will be less rapid for more anisotropic wave modes, it can be expected to be significant.

Eq. (40), on the other hand, has real or imaginary characteristic surfaces depending on the wave frequency. For frequencies for which the characteristics are real, the problem is said to be hyperbolic. The waves associated with real characteristics do not propagate isotropically; they are subject to shocks and discontinuities. In this linear problem, the shocks or discontinuities propagate only along the characteristics, as do any discontinuities in the derivatives.

Even when Eq. (40) has real characteristics, there are real and imaginary characteristics in the same equation. The effect of this coupling will be examined later when we obtain explicit solutions. Except to the extent that the waves associated with imaginary characteristics are driven by waves associated with real characteristics, they will not be treated in detail in this paper. Such waves would be worth a separate investigation.

The solution of Eq. (40), obtained by the method of characteristics, is $\phi =$ constant along the surfaces defined by

$$dx = \pm \sqrt{(\epsilon_P/\epsilon_0)} dz. \quad (41)$$

The coefficients ϵ_0 and ϵ_P can each be positive and negative as a function of fre-

quency. The condition that the characteristics are real is

$$\epsilon_P(\omega)/\epsilon_0(\omega) > 0. \quad (42)$$

For a plasma composed of a single type of positive ion, a simple analysis gives the signs of ϵ_P and ϵ_0 :

$$0 < \omega < \Omega_i ; \epsilon_P < 0$$

$$\Omega_i < \omega < \Omega_{LC} ; \epsilon_P > 0$$

$$\Omega_{LC} < \omega < \Omega_e ; \epsilon_P < 0$$

$$\Omega_e < \omega < \Omega_{UC} ; \epsilon_P > 0$$

$$\Omega_{UC} < \omega < \infty ; \epsilon_P < 0$$

$$0 < \omega < \omega_p ; \epsilon_0 < 0$$

$$\omega_p < \omega < \infty ; \epsilon_0 > 0$$

Here, Ω_i and Ω_e represent the ion and electron gyrofrequencies, while

$$\Omega_{UC, LC}^2 = (1/2)[\Omega_e^2 + \Omega_i^2 + \omega_p^2 \pm \sqrt{(\Omega_e^2 - \Omega_i^2 + \omega_{pe}^2 - \omega_{pi}^2)^2 + 4\omega_{pe}^2\omega_{pi}^2}] \quad (43)$$

are the upper and lower cut-off frequencies. Ω_{UC} and Ω_{LC} are just the zeroes of ϵ_P .

Table 1. Frequencies for Which There Are Real Characteristics

$0 < \omega < \Omega_i$	real	hyperbolic
$\Omega_i < \omega < \Omega_{LC}$	imaginary	elliptic
$\Omega_{LC} < \omega < \Omega_e$	real	hyperbolic
$\Omega_e < \omega < \omega_p$	imaginary	elliptic
$\omega_p < \omega < \Omega_{UC}$	real	hyperbolic
$\Omega_{UC} < \omega < \infty$	imaginary	elliptic

Based on these results, the frequencies for which there are real characteristics can be determined (Table 1). We have tacitly assumed the ordering $\Omega_e^2 \ll \omega_p^2$, typical of the low Earth-orbit environment. There are three regions that can support shock-like disturbances: (1) Alfvén--below the ion gyrofrequency, (2) whistler--between the lower cutoff frequency and the electron gyrofrequency, and (3) upper hybrid--between the plasma frequency and the upper cutoff frequency. In these regions, the angle between the characteristics and the magnetic field is

$$\theta = \pm \tan^{-1} \sqrt{(\epsilon_p / \epsilon_0)}. \quad (44)$$

The angle θ is shown in Figure 1 for a plasma typical of low-altitude Earth

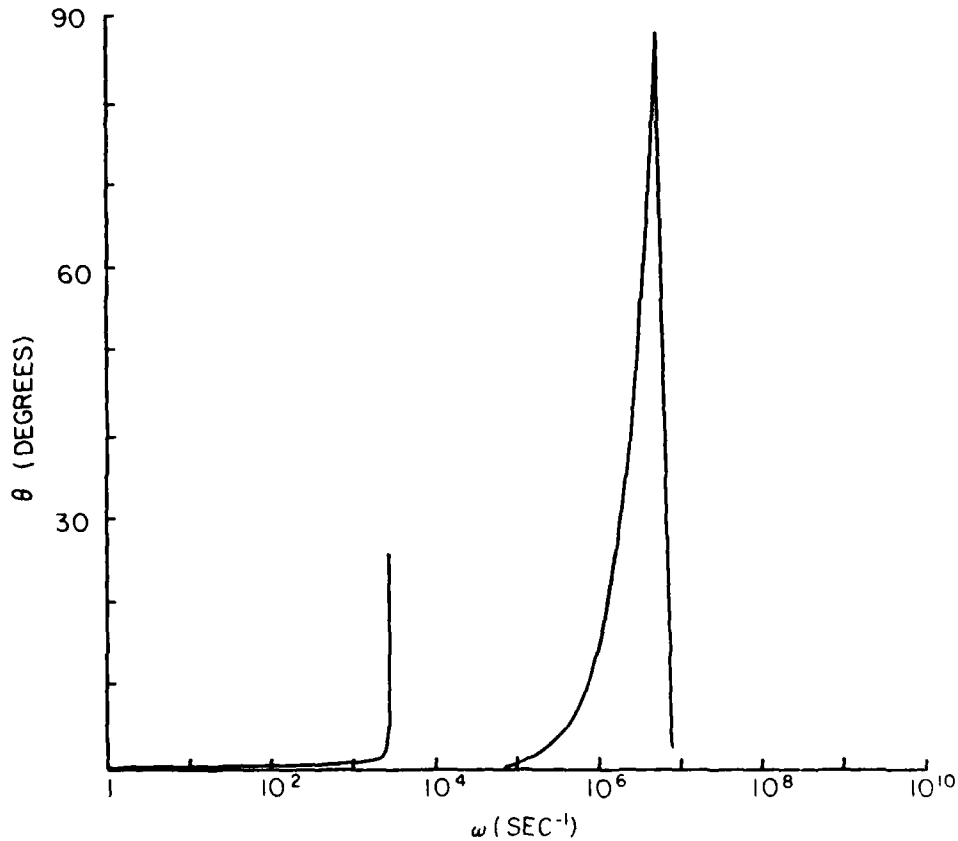


Figure 1. The Angle Between the Characteristics and the Magnetic Field, Given as a Function of Wave Frequency, for a Hydrogen Plasma With $n = 10^4 \text{ cm}^{-3}$ and $B = 0.3 \text{ G}$.

orbit: a hydrogen plasma with $n = 10^4 \text{ cm}^{-3}$ and $B = 0.3 \text{ G}$. In order of increasing frequency, the three curves represent the characteristics associated with the Alfvén, whistler, and upper hybrid regions. At very low frequencies, the angle is essentially zero, the well known result for Alfvén waves: Alfvén waves propagate only along the field. The angle broadens as the frequency increases and becomes 90° at the ion gyrofrequency. This behavior repeats above Ω_{LC} : the angle is zero at Ω_{LC} and increases to 90° at the electron gyrofrequency. Above the plasma frequency, the behavior is reversed: the angle is 90° and decreases to zero at Ω_{UC} . The discussion of the behavior of the waves with respect to these angles is deferred to a later section.

3.1 Propagation of Discontinuities

The above discussion of the existence of discontinuities originated with the formal mathematical treatment of the characteristics, which is quite abstract at best. The present section is designed to show the relation of the characteristics to the discontinuities. The treatment is not general, but is much more direct and physical.

To treat discontinuities, we start with Eqs. (16) through (18) for the electric field components. It follows from Eqs. (16) and (18) that

$$\partial_x(-\epsilon_P \delta E_x + \epsilon_H \delta E_y) + \partial_z(\epsilon_0 \delta E_z) = 0. \quad (45)$$

This is a divergence equation. Discontinuities can be treated by integrating over a Gaussian pillbox surface enclosing the discontinuity and using the divergence theorem

$$\int \vec{\nabla} \cdot \vec{A} d^3x = \oint \vec{n} \cdot \vec{A} da. \quad (46)$$

For a jump discontinuity, Eq. (46) shows that the normal component of the vector \vec{A} is continuous:

$$[A_n] = 0. \quad (47)$$

The bracket notation is defined by

$$[Q] \equiv Q_2 - Q_1 \quad (48)$$

where Q is any quantity and 1 and 2 refer to the two different sides of the discontinuity.

Applying this method to Eq. (45), we obtain

$$n_x [-\epsilon_P \delta E_x + \epsilon_H \delta E_y] + n_z [\epsilon_0 \delta E_z] = 0. \quad (49)$$

Assuming that the coefficients ϵ are continuous, we have

$$-n_x \epsilon_P [\delta E_x] + n_x \epsilon_H [\delta E_y] + n_z \epsilon_0 [\delta E_z] = 0. \quad (50)$$

In a similar manner, it follows from Faraday's Law (see Eqs. (19) and (24) that

$$n_z [\delta E_x] - n_x [\delta E_z] = 0 \quad (51)$$

$$[\delta E_y] = 0. \quad (52)$$

The only solutions of Eqs. (50), (51), and (52) for which the electric field discontinuities do not vanish are given by

$$n_x^2 \epsilon_P - n_z^2 \epsilon_0 = 0 \quad (53)$$

or

$$n_x = \pm \sqrt{(\epsilon_0 / \epsilon_P)} n_z. \quad (54)$$

The normal vector is perpendicular to the surface of discontinuity, and, by Eq. (44), perpendicular to a characteristic surface. It follows that any discontinuities in the electric field must lie on a characteristic surface. It further follows that there are no discontinuities at all unless the characteristics are real.

3.2 Phase and Group Velocities

Since the methods developed here use the same assumptions as a more orthodox plane wave treatment of plasma waves, it is to be expected that the important features should be the same. This is the case in several respects. In particular, the characteristics can be identified as the resonance lines of the plane wave picture. The purpose of this section is to provide a physical picture of the characteristics as resonances to aid in the development of the idea of the characteristics as carriers of discontinuities.

The dispersion relation of cold plasma waves can be obtained from any of the

principal equations: Eqs. (16), (17), and (18), Eqs. (27) and (28), or Eq. (36). It is convenient to write it in the form

$$D(\omega, \vec{k}) = a/k^4 + b/k^2 + c = 0 \quad (55)$$

where the coefficients are defined by

$$a = \epsilon_0 (\epsilon_P^2 + \epsilon_H^2) \quad (56)$$

$$b = 2\epsilon_0 \epsilon_P \cos^2 \psi + (\epsilon_0 \epsilon_P - \epsilon_P^2 - \epsilon_H^2) \sin^2 \psi \quad (57)$$

$$c = \epsilon_0 \cos^2 \psi - \epsilon_P \sin^2 \psi \quad (58)$$

and ψ is the angle between \vec{k} and \vec{B} .

To investigate the relation of resonances to the characteristics, we inquire about the behavior of the phase and group velocities when the wave vector is perpendicular to the characteristics. If \vec{k} is perpendicular to one of the characteristics, defined by Eq. (44), then

$$\tan^2 \psi = 1/\tan^2 \theta = \epsilon_0 / \epsilon_P \quad (59)$$

so that

$$c = 0 \quad (60)$$

which shows that the characteristics are resonance lines (see Stix, p. 14) and

$$b = \epsilon_0 (\epsilon_0 \epsilon_P + \epsilon_P^2 - \epsilon_H^2) / (\epsilon_0 + \epsilon_P). \quad (61)$$

Then the roots of the dispersion relation are

$$1/k^2 = 0 \quad (62)$$

and

$$1/k^2 = -b/a. \quad (63)$$

We conclude that when \hat{k} is perpendicular to a characteristic, the associated wave vector, given by Eq. (62), is infinite and the phase velocity is

$$V_{ph} = \omega/k = 0. \quad (64)$$

Let us pursue the same line of thought with the group velocity. The group velocity is defined to be

$$\hat{V}_g = -(\partial D / \partial \hat{k}) / (\partial D / \partial \omega). \quad (65)$$

The numerator is

$$\partial D / \partial \hat{k} = \hat{e}_k (\partial D / \partial k) + (\hat{e}_\psi / k) (\partial D / \partial \psi) \quad (66)$$

where the unit vectors \hat{e}_k and \hat{e}_ψ are parallel and perpendicular to \hat{k} , respectively. Evaluated at $c(\psi) = 0$, so that \hat{k} is perpendicular to a characteristic,

$$V_{gk} = 2b / (k^3 \partial c / \partial \omega) = 0 \quad (67)$$

$$V_{g\psi} = -(\partial c / \partial \psi) / (k \partial c / \partial \omega) = 0 \quad (68)$$

so that the group velocity vanishes. At the same time, the group velocity is along the characteristic

$$V_{gk} / V_{g\psi} = -2b / (k^2 \partial c / \partial \psi) = 0. \quad (69)$$

From this, we may draw a physical picture of the role of the characteristics. Plane waves emitted by a localized source, for which \hat{k} is perpendicular to a characteristic, do not propagate across the characteristic. Both the phase velocity and group velocity vanish, and so the waves may accumulate along the characteristic. For a sufficiently steady situation (long-lived source plus steady background plasma), the waves may build up to any arbitrary amplitude within the context of the linear approximation. Because the points in space just across the characteristics are not causally related to those on the side occupied by the disturbance, this disturbance may form a shock wave of arbitrary amplitude. Since the plane waves are supposed to extend an indefinite distance from the source, the shock wave can extend to large distances from the source.

From the above discussion, we can make clear what we mean by "shock-like disturbance," a term used throughout this paper. An observer passing through a characteristic or resonant surface associated with a particular frequency would measure a sudden jump in the power at that frequency: the power would be zero on one side and finite on the other. However, since the characteristics themselves are frequency-dependent, the disturbance associated with a band of frequencies has a finite width: the medium is dispersive. Such a disturbance is quite unlike the Cherenkov cone or sonic boom associated with nondispersive light waves or sound waves (or fast mode waves, for that matter); these shocks show a sudden jump in power across a single shock surface at all frequencies.

Eq. (69) will be important in the analysis of analytic solutions. It can be written as

$$V_{gk}/V_{g\psi} = \sqrt{(\epsilon_0/\epsilon_P) \epsilon_*/k^2} \quad (70)$$

where

$$\epsilon_* = (\epsilon_0 \epsilon_P + \epsilon_P^2 - \epsilon_H^2)/(\epsilon_0 + \epsilon_P). \quad (71)$$

From Eq. (70), it follows that when $\epsilon_* < 0$, the group velocity is inside the characteristics, while when $\epsilon_* > 0$, the group velocity is outside the characteristics. "Inside" and "outside" here mean "toward the field direction" and "away from the field direction," respectively. This distinction will lead to two separate classes of shock-like disturbances caused by spacecraft corresponding to spacecraft velocity essentially across the field and along the field, respectively. There will also be two different ways for waves excited by spacecraft to spread: along the field and across the field, respectively.

The results of this section can be illustrated in the limit of low-frequency waves for which solutions can be obtained analytically. We state the following without proof. In the limit of low frequency, the characteristics are determined by the equation

$$[\partial_z^2 - (\omega^2/\omega_{gm}^2) \partial_x^2 - \omega^2/V_A^2] \delta B_y = 0 \quad (72)$$

where the geometric mean frequency (see Stix,¹ p. 32) is defined by

$$\omega_{gm}^2 = \Omega_e \Omega_i. \quad (73)$$

The phase velocity is

$$\omega^2/k^2 = v_A^2 [\cos^2 \psi - (\omega^2/\omega_{gm}^2) \sin^2 \psi]. \quad (74)$$

The directions of the group and phase velocities are related by

$$\tan \psi_g = -(\omega^2/\omega_{gm}^2) \tan \psi. \quad (75)$$

The square of the group velocity is

$$v_g^2 = v_A^2 [\cos^2 \psi_g - (\omega_{gm}^2/\omega^2) \sin^2 \psi_g] / \cos^4 \psi_g. \quad (76)$$

The phase velocity goes to zero at

$$\tan \psi = \pm \omega_{gm}/\omega \quad (77)$$

and the group velocity goes to zero at

$$\tan \psi_g = \pm \omega/\omega_{gm}. \quad (78)$$

Because the angles between the characteristics and field are

$$\theta = \pm \tan^{-1}(\omega/\omega_{gm}), \quad (79)$$

the main results of this section follow easily. When \vec{k} is perpendicular to a characteristic, the phase velocity is zero [Eq. (74)], the group velocity is along the characteristic [Eq. (78)], and the group velocity is zero [Eq. (76)]. The phase and group velocities are shown in Figure 2, along with the characteristics. We show $\omega/\omega_{gm} = 0.2$ for purposes of clarity. In fact, the low-frequency approximation used requires $\omega \ll \Omega_i$ or $\omega/\omega_{gm} \ll \sqrt{m_e/m_i} \sim 0.023$. The magnetic field in the figure is vertical, as indicated by the arrow.

We note that Eq. (76) is different from the results illustrated by Musielak.² His low-frequency group velocity loci do not go to zero at any angle.

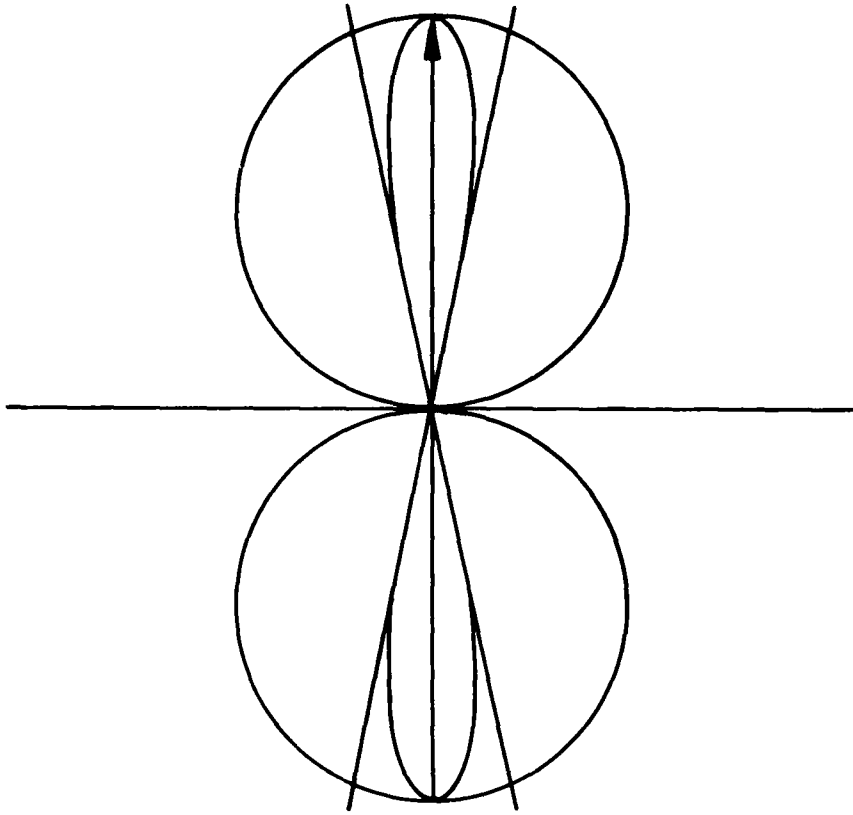


Figure 2. The Phase and Group Velocities of Low Frequency Plasma Waves, Given as Functions of Angle With Respect to the Magnetic Field. The direction of the magnetic field is indicated by the arrow. The characteristics are also plotted. The angle between the characteristics and the magnetic field is exaggerated for clarity.

1. PROGRESSING WAVE SOLUTIONS

With the discussion of the characteristics and the propagation of discontinuities as background, we now turn to solutions of the equations. It is well known that equations such as Eqs. (25) and (26) or (36) can be solved by the method of progressing waves (see Courant and Hilbert,⁵ Chap. VI). For the present purposes, we will find approximate solutions of Eqs. (27) and (28). To do this, we look for solutions of the form

$$\alpha = \sum_{n=0}^{\infty} [\delta^{(n)}(\mu) e_{n\mu}(\mu, \nu) + \delta^{(n)}(\nu) e_{n\nu}(\mu, \nu)] \quad (80)$$

$$\beta = \sum_{n=0}^{\infty} [\delta^{(n)}(\mu) b_n(\mu, \nu) + \delta^{(n)}(\nu) d_n(\mu, \nu)] \quad (81)$$

where μ and ν are the characteristics

$$\mu = z + \sqrt{(\epsilon_0/\epsilon_P)}x \quad (82)$$

$$\nu = z - \sqrt{(\epsilon_0/\epsilon_P)}x \quad (83)$$

[see Eq. (41)]. In Eqs. (80) and (81), $\delta^{(0)}(x)$ is the Dirac delta function, $\delta^{(n)}(x)$ is its n th derivative when $n < 0$, and

$$\begin{aligned} \delta^{(n)}(x) &= x^n/n!, \quad x > 0 \\ &= 0, \quad x < 0 \end{aligned} \quad (84)$$

when $n > 0$. Because of the Fourier transform in time, the delta function indicates a source oscillating at frequency ω . Because of the form of the expansions (80) and (81), the disturbance is assumed to vanish outside the characteristics.

The results to be derived below hold only for a source at rest in the proper frame of the plasma. This restriction arises because of our treatment in configuration space rather than Fourier space. While the Doppler shifts associated with moving sources are easily treated in Fourier space, the reversion to configuration space represents an intractable analytical problem. It is possible to treat it numerically, however. Remarks about moving sources are deferred until later sections.

The treatment that we have outlined does not properly treat the source currents associated with the spacecraft interaction that cause the fluctuations. To do so here would unduly complicate the presentation. The equations with source terms are listed in the Appendix, along with a discussion of the modifications required to use them.

Substitution of Eqs. (80) and (81) into Eqs. (27) and (28) followed by the equating to zero of the coefficient of each $\delta^{(n)}(\mu)$ leads to the recursion relations

$$b_0 = 0 \quad (85)$$

$$b_1 + 2(\partial_\mu - \partial_\nu)b_0 = 0 \quad (86)$$

$$(1 + \epsilon_0/\epsilon_P)[b_i + 2(\partial_\mu - \partial_\nu)b_{i-1} + 2(\partial_\mu - \partial_\nu)^2 b_{i-2}] - \epsilon_P b_{i-2} + \epsilon_H a_{i-2} = 0, i > 1 \quad (87)$$

$$-(\epsilon_H/\epsilon_P)b_1 + \partial_\nu a_0 - 2(\epsilon_H/\epsilon_P)(\partial_\mu - \partial_\nu)b_0 = 0 \quad (88)$$

$$-(\epsilon_H/\epsilon_P)b_i + \partial_\nu a_{i-1} - 2(\epsilon_H/\epsilon_P)(\partial_\mu - \partial_\nu)b_{i-1} + \partial_\mu \partial_\nu a_{i-2} - \epsilon_P a_{i-2} - \epsilon_H b_{i-2} + (\partial_\mu - \partial_\nu)^2 b_{i-2} = 0, i > 1 \quad (89)$$

The recursion relations for c_n and d_n are entirely similar and can be obtained by interchanging a and c , b and d , and μ and ν . To specify the solution, we choose

$$a_0(0, \nu) = 1 \quad (90)$$

$$a_1(0, \nu) = 0, i > 0. \quad (91)$$

This choice implied that α is a delta function at $\mu = 0, \nu = 0$. The meaning of the solution with these initial conditions is that it represents the manner in which the disturbance that results from an oscillating point source propagates. The solutions for these initial conditions are

$$a_0 = 1 \quad (92)$$

$$a_1 = \epsilon_* \nu \quad (93)$$

$$a_2 = (1/2)(\epsilon_* \nu)^2 \quad (94)$$

$$a_3 = (1/3!)(\epsilon_* \nu)^3 - [(\epsilon_H^2 \epsilon_P)/(\epsilon_0 + \epsilon_P)] \nu \quad (95)$$

$$b_0 = 0 \quad (96)$$

$$b_1 = 0 \quad (97)$$

$$b_2 = -\epsilon_P \epsilon_H / (\epsilon_0 + \epsilon_P) \quad (98)$$

$$b_3 = - [\epsilon_P \epsilon_H / (\epsilon_0 + \epsilon_P)] (\epsilon_* \nu) \quad (99)$$

$$b_4 = -\epsilon_H [(1/2)(\epsilon_* \nu)^2 + (2\epsilon_0 \epsilon_P + 3\epsilon_P^2 - 2\epsilon_H^2) / (\epsilon_0 + \epsilon_P)] \quad (100)$$

where

$$\epsilon_* = (\epsilon_0 \epsilon_P + \epsilon_P^2 - \epsilon_H^2) / (\epsilon_0 + \epsilon_P). \quad (101)$$

From these terms, it is possible to describe the nature of the solution. The delta function

$$\alpha = (1 + \epsilon_P / \epsilon_0) \delta B_y - (\epsilon_H / \epsilon_0) \delta B_x = \delta(\mu) \quad (102)$$

lies along the characteristic line $\mu = 0$, that is, along $z = -\sqrt{(\epsilon_0 / \epsilon_P)}x$. There is no corresponding delta function in $\beta - (1 + \epsilon_P / \epsilon_0) \delta B_x + (\epsilon_H / \epsilon_0) \delta B_y$. There are, however, delta functions in both δB_y and δB_x .

The coefficient a_1 represents the jump in α across $\mu = 0$. This jump, which is initially zero (because of our choice of initial conditions), grows linearly with distance away from the source. Again, there is no jump in β , but there are jumps in both δB_y and δB_x . The coefficient a_2 represents the jump in the first derivative of α ; it grows quadratically away from the source. The jump in the first derivative of β does not grow quadratically near the spacecraft, however. Eq. (98) shows that the jump in the first derivative of β is discontinuous, even at the origin.

The nature of the solutions is that of coupled waves. The coupling, as mentioned in connection with Eqs. (34) and (35), is determined by ϵ_H . When ϵ_H goes to zero, the solutions for the a_n and b_n are

$$a_n = (\epsilon_P \nu)^n / n! \quad (103)$$

$$b_n = 0. \quad (104)$$

Summing the series (86) and (81), we have

$$\begin{aligned} \alpha &= 2 \sum_{n=0}^{\infty} (\epsilon_P \mu \nu)^n / (n!)^2 \\ &= 2J_0 [\sqrt{-2\epsilon_P \mu \nu}] \end{aligned} \quad (105)$$

where $J_0(z)$ is the Bessel function and

$$\beta = 0. \quad (106)$$

The factor of 2 in Eq. (105) appears because of the contributions of the c_n in Eq. (80). Eq. (105) is the well known fundamental solution of Eq. (34).

From this discussion, it appears that the first few terms of α are the same as

$$\alpha = J_0[\sqrt{(-2\epsilon_*\mu\nu)}], \quad \epsilon_* < 0 \quad (107)$$

and that modifications appear because of mode coupling in a_3 , b_2 , and higher order terms. The former result is easy to prove. By eliminating the low order terms in the recursion relations, so that they reduce to

$$(1 + \epsilon_0/\epsilon_P)b_i + \epsilon_H a_{i-2} + \dots = 0 \quad (108)$$

$$a_{i-1} - (\epsilon_H/\epsilon_P)b_i - \epsilon_P a_{i-2} + \dots = 0, \quad (109)$$

one immediately obtains

$$\partial_\nu a_{i-1} = \epsilon_* a_{i-2} + \dots \quad (110)$$

so that α is

$$\alpha = J_0[\sqrt{(-2\epsilon_*\mu\nu)}] + \dots, \quad \epsilon_* < 0 \quad (111)$$

where the ellipsis represents the remaining terms that arise because of the coupling.

In contrast to the low-frequency Alfvén waves, the solution for higher frequency waves depends on the sign of ϵ_* . If $\epsilon_* > 0$, it would appear that

$$\alpha = I_0[\sqrt{(2\epsilon_*\mu\nu)}] + \dots, \quad \epsilon_* > 0 \quad (112)$$

where $I_0(z)$ is the modified Bessel function. The asymptotic form of Eq. (112) for large argument is

$$\alpha = e^{\zeta} / \sqrt{2\pi\zeta} + \dots, \epsilon_* > 0 \quad (113)$$

where $\zeta = -2\epsilon_*\mu\nu$, which would suggest an exponential increase in the wave amplitude with z .

Such exponential behavior presumably does not occur for the following reason: In Eq. (70), we saw that the sign of ϵ_* determined the side of the characteristics upon which the waves could propagate. If $\epsilon_* > 0$, the waves propagate outside (away from the field) of the characteristics, while the form of Eqs. (80) and (81) assumes that the disturbance propagates inside and vanishes outside. The intuitively correct result is obtained by replacing the delta functions of Eqs. (80) and (81) by $\delta^{(n)}(-\mu)$ and $\delta^{(n)}(-\nu)$ if $\epsilon_* > 0$. With an assumed solution of this form, the sign of μ or ν (but not both) is flipped in each expansion with coefficients a_n and c_n . The result is that

$$\alpha = J_0[\sqrt{(-2\epsilon_*\mu\nu)}] + \dots, \epsilon_* > 0 \quad (114)$$

that is, the solution is of the same form as Eq. (111) but vanishes inside the characteristics.

The behavior of ϵ_* in regions where real characteristics exist, is shown in Figure 3 for the same low Earth orbit conditions as Figure 1. Note that $\epsilon_* < 0$ in the Alfvén and whistler regions and $\epsilon_* > 0$ in the upper hybrid region.

It should be noted that the correspondence of "inside" and "outside" with the sign of ϵ_* was a purely local result; it did not determine whether the group velocity was always inside or outside of the characteristics. Because of the complicated nature of the group velocity loci, and the fact that the group velocity along or across the field is not related to ϵ_* , such a determination would presumably have to come from a numerical search. So we are faced with the following alternatives: Either our correspondence is correct, or the wave amplitudes can grow exponentially with distance near the spacecraft. While the existence of growing waves would be surprising, it is not impossible. Even though the driving I_0 term grows rapidly near the spacecraft, the remaining terms could easily conspire to reduce it at great distances. Because of the hyperbolic nature of the problem, there is no boundary condition far from the spacecraft which can be used to eliminate this solution. The only apparent constraint is that the asymptotic wave amplitudes are nondecreasing. This is essentially an energy conservation argument: If the asymptotic wave amplitudes continued to grow, the steady source could not provide sufficient energy to sustain them. Nor could the cold plasma provide the energy, as it is known to be stable. It would be a worthwhile exercise to look for such waves;

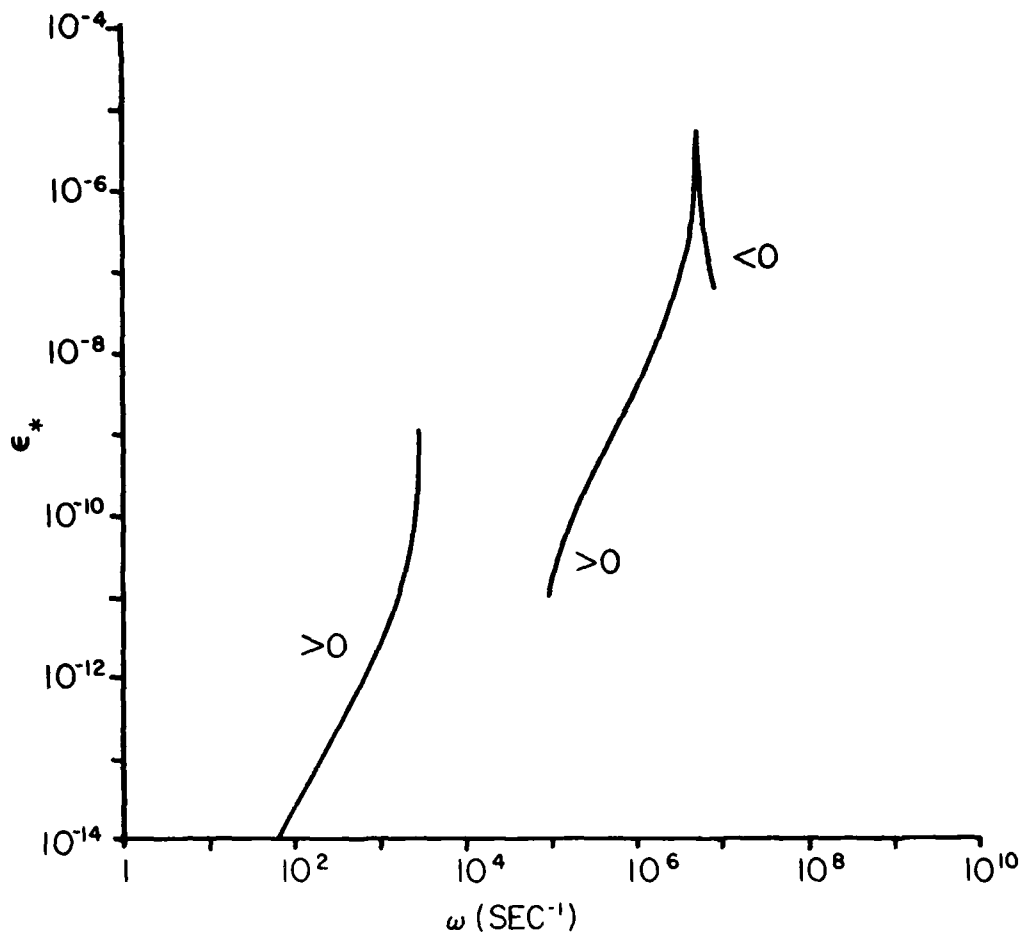


Figure 3. The Parameter ϵ_* Plotted as a Function of Wave Frequency. The properties of the plasma are the same as Figure 1. In the Alfvén region ($\omega < 2 \times 10^3 \text{ sec}^{-1}$) and the whistler region ($10^5 < \omega < 7 \times 10^6$) ϵ_* is negative. In the upper hybrid region ($8 \times 10^6 < \omega$) ϵ_* is positive

they could provide a source of extremely rapid spatial wave growth near the spacecraft.

Several remarks should be made about the nature of these solutions.

(1) Despite the fact that the solutions are analytic, they can only be regarded as qualitative; they are presented only for the purpose of identifying typical physical features.

(2) The solutions are only two-dimensional; solutions can change significantly when the dimensionality of the problem is changed. The best known example is

light: three-dimensional solutions are delta functions, while two-dimensional solutions are Bessel functions. While both have sharp wave fronts, the two-dimensional solutions have trailing wakes entirely missing in three dimensions.

(3) The solutions of this section are for delta function disturbances in the magnetic field. A better physical description would be the solutions for a delta function current source. (For further details, see the Appendix.)

(4) The squares of the results of this section represent the spectral power density of the fluctuations resulting from a two-dimensional source stationary in the proper frame. For applications, the power spectral density should be calculated for specified current sources (see Appendix).

5. STEADY PLASMA STRUCTURE AROUND A MOVING SOURCE

The present section is somewhat outside the main line of development and can be omitted on a first reading. The purpose is to develop a formal method for calculating the steady plasma structure around a moving source. Because of the intractable analytic nature of the result, we have computed results only in two simple cases. However, these cases are instructive and may help the uninitiated reader to make contact with the subject. The formal results include the entire steady radiation field, which has contributions from waves of all frequencies. As such, it should be able to serve as a useful starting point in future investigations. In contrast to the rest of this paper, the results of this section are fully three-dimensional.

The problem that we wish to investigate is the plasma response to a source of current moving with constant velocity, \vec{U} . Let the source be characterized by a charge density, η , so that a point source can be represented by

$$\vec{J} = \eta \vec{U} = \vec{U} \delta(x - \vec{U}t). \quad (115)$$

We wish to use this source current to calculate a Green's function, and so have chosen $\eta = 1$. The Ampere-Faraday Law is

$$\vec{\nabla} \times (\vec{\nabla} \times \delta \vec{E}) = \epsilon_{ij} \delta \vec{E}_j + (4\pi i \omega / c^2) \vec{J} \quad (116)$$

where the ϵ_{ij} represent the coefficients defined in Eq. (10). Without working out the details, one can see that the general form of the spatial Fourier transform of Eq. (116) is

$$A_{ij} \delta E_j = (4\pi i \omega / c^2) J_i \quad (117)$$

where A is a matrix whose elements depend on \vec{k} and $\epsilon_{ij}(\omega)$. The solution for $\delta \vec{E}$ is

$$\delta E_i = (4\pi i \omega / c^2) A_{ij}^{-1} J_j \quad (118)$$

where the inverse matrix A^{-1} is given by

$$A_{ij}^{-1} = a_{ij}(\omega, \vec{k}) / D(\omega, \vec{k}). \quad (119)$$

Here, the $a_{ij}(\omega, \vec{k})$ are coefficients resulting from the inversion; they depend on ω through the $\epsilon_{ij}(\omega)$. $D(\omega, \vec{k})$ is the dispersion function; the dispersion relation is $D(\omega, \vec{k}) = 0$. The Fourier transform of the Green's function for this point source is

$$G_i(\omega, \vec{k}) = (4\pi i \omega / c^2) [a_{ij}(\omega, \vec{k}) / D(\omega, \vec{k})] J_j(\omega, \vec{k}) \quad (120)$$

where $J_i(\omega, \vec{k})$ is the Fourier transform of the current density given by Eq. (115) and is given explicitly by

$$J_i(\omega, \vec{k}) = [U_i / (2\pi)^3] \delta(\omega - \vec{k} \cdot \vec{U}). \quad (121)$$

Then the Green's function is

$$G_i(t, \vec{x}) = \int d^3k d\omega G_i(\omega, \vec{k}). \quad (122)$$

After some easy steps, the Green's function can be written symbolically in the form

$$G_i(\vec{x} - \vec{U}t) = \theta_i \int d^3k [\exp(i\vec{k} \cdot (\vec{x} - \vec{U}t))] / D(\vec{k} \cdot \vec{U}, \vec{k}) \quad (123)$$

where θ_i is an operator defined by

$$\theta_i = [U_i / (2\pi^2 c^2)] (\vec{U} \cdot \vec{\nabla}) a_{ij}(-i\vec{U} \cdot \vec{\nabla}, -i\vec{\nabla}). \quad (124)$$

Note that a_{ij} depends on $\vec{U} \cdot \vec{\nabla}$ through the dependence of the ϵ_{ij} on ω . It is a complicated function of differential operators. Its evaluation normally involves power series of operators.

Several remarks about Eq. (124) are appropriate:

- (1) The wave pattern is stationary in the frame in which the source is at rest.
- (2) There are two principal pieces to the Green's function: the operator O_1 and the radiation integral

$$R = \int d_3k [\exp(i\vec{k} \cdot (\vec{x} - \vec{U}t))] / D(\vec{k} \cdot \vec{U}, k). \quad (125)$$

- (3) The radiation integral carries the fundamental information about the expansion of the wave: phase speeds, group speeds, characteristics, and disturbance topology.

- (4) The details of each wave amplitude are determined by the operator O_1 .

- (5) R is simply the spatial Fourier transform of the inverse dispersion function.

- (6) R depends on all wave frequencies because of the Doppler shift, represented through the dependence of D on $\vec{k} \cdot \vec{U}$.

Eq. (123) is difficult or impossible to evaluate in any general way. We would like to illustrate its use through a simple evaluation of R for two special cases: (1) fast mode waves, and (2) MHD Alfvén waves. To do so, we shall drop all constant factors and derivatives, which are inessential.

- (1) The fast mode dispersion relation is

$$D(\omega, \vec{k}) = \omega^2 - k^2 V_A^2 \quad (126)$$

so that

$$D(\vec{k} \cdot \vec{U}, k) = (\vec{k} \cdot \vec{U})^2 - k^2 V_A^2. \quad (127)$$

To proceed, let $\vec{U} = (U_x, 0, 0)$ so that the velocity is perpendicular to the field. Then

$$D(\vec{k} \cdot \vec{U}, k) \sim k_x^2 - (k_y^2 + k_z^2) / (U^2 / V_A^2 - 1). \quad (128)$$

In carrying out the transforms in Eq. (123), there are two cases to consider. If $U^2 / V_A^2 > 1$, D has two real roots for k_x . Carrying out the transform in the usual way, we obtain

$$R \sim 1/\sqrt{[x^2 / (U^2 / V_A^2 - 1) - y^2 - z^2]} \text{ if } y^2 + z^2 < x^2 / (U^2 / V_A^2 - 1)$$

= 0, otherwise

This represents a fast mode shock for the case that the source speed exceeds the Alfvén speed. The disturbance vanishes outside the shock cone, shows a sudden jump at the shock cone, and is nonzero inside. This is just Cherenkov radiation in a cold plasma.

If $U^2/V_A^2 < 1$, there are two imaginary roots of k_x . In this case, the radiation integral is

$$R \sim 1 / [x^2 / (1 - U^2/V_A^2) + y^2 + z^2]. \quad (130)$$

This has the same form as Eq. (129) except that there is no shock cone.

(2) The MHD Alfvén mode dispersion relation is

$$D(\omega, \vec{k}) = \omega^2 - (\vec{k} \cdot \vec{V}_A)^2 \quad (131)$$

so that

$$D(\vec{k} \cdot \vec{U}, \vec{k}) = (\vec{k} \cdot \vec{U})^2 - (\vec{k} \cdot \vec{V}_A)^2. \quad (132)$$

With the velocity again in the x-direction

$$D(\vec{k} \cdot \vec{U}, \vec{k}) = k_x^2 U^2 - k_z^2 V_A^2. \quad (133)$$

Evaluation of the integrals then leads to

$$R \sim \delta(y) [\delta(x + Uz/V_A) + \delta(x - Uz/V_A)]. \quad (134)$$

This solution is just two delta functions in opposite directions along the field: they are the Alfvén wings for a point source. They are tilted by an angle $\tan^{-1}(U/V_A)$ with respect to the field and lag behind the source.³

6. APPLICATIONS TO SPACECRAFT

Up to this point, we have developed several apparently disparate approaches to our problem. It is time to try to unify them into one coherent picture. The main difficulty we face is to incorporate the motion of the spacecraft into our results. Aside from the last section, the results are valid only for sources which

are stationary in the proper frame of the plasma. For such a motionless source, the methods outlined above should provide a detailed accounting of the behavior of waves and disturbances propagating away from the source.

What is required is a generalization of the characteristics that applies to the wave field of moving sources. These characteristics should be the carriers of discontinuities that originate at the spacecraft. The spatial methods that have been developed above are not particularly helpful for the following reasons: The characteristics in the proper frame do not depend on the group velocity because, as we have seen, it becomes zero at the characteristics. On the other hand, the spatial characteristics in a flowing plasma must have some relation to the group velocity. Another way of looking at it is that the angle of the characteristics in the frame of the moving source must be determined by the ratio of some speed in the problem to the source speed, U . This is true in any frame; if the source is stationary in the proper frame, the source velocity and the group velocity associated with the characteristics are both zero.

The appropriate generalization has been known for a long time (see Jeffrey and Taniuti,⁶ p. 186). If $\vec{V}_g - \vec{U}$ is tangent to the group velocity surface, then the direction $\vec{V}_g - \vec{U}$ is characteristic:

$$(\vec{V}_g - \vec{U}) \cdot \vec{\nabla} \phi = 0 \quad (135)$$

that is, the convected group velocity is parallel to the characteristic surface. The construction of the characteristics is shown in Figure 4; we have used the group velocity of Figure 2 in this example. The magnitude of the spacecraft velocity has been greatly exaggerated for clarity.

The characteristics determined in this way satisfy the usual requirement that characteristic surfaces be the carriers of discontinuities. This is easy to see from the significance of the group velocity. The characteristics here are just the envelope of the group velocity and so determine the limits past which a localized fluctuation cannot spread: inside the characteristic surface, the disturbance does not vanish, while outside, it does.

For further details, see Jeffrey and Taniuti.⁶ For the present purposes, it is sufficient to note the following: Spacecraft velocities are about 8 km/sec or less while typical group velocities are on the order of the Alfvén speed, several hundred kilometers per second or more. Unless there are group velocities less than the spacecraft velocity, then no new qualitative features (that is, new characteristic surfaces) will occur. In that case, the analysis of this paper can be used to

6. Jeffrey, A., and Taniuti, T. (1964) Non-Linear Wave Propagation, Academic Press, New York.

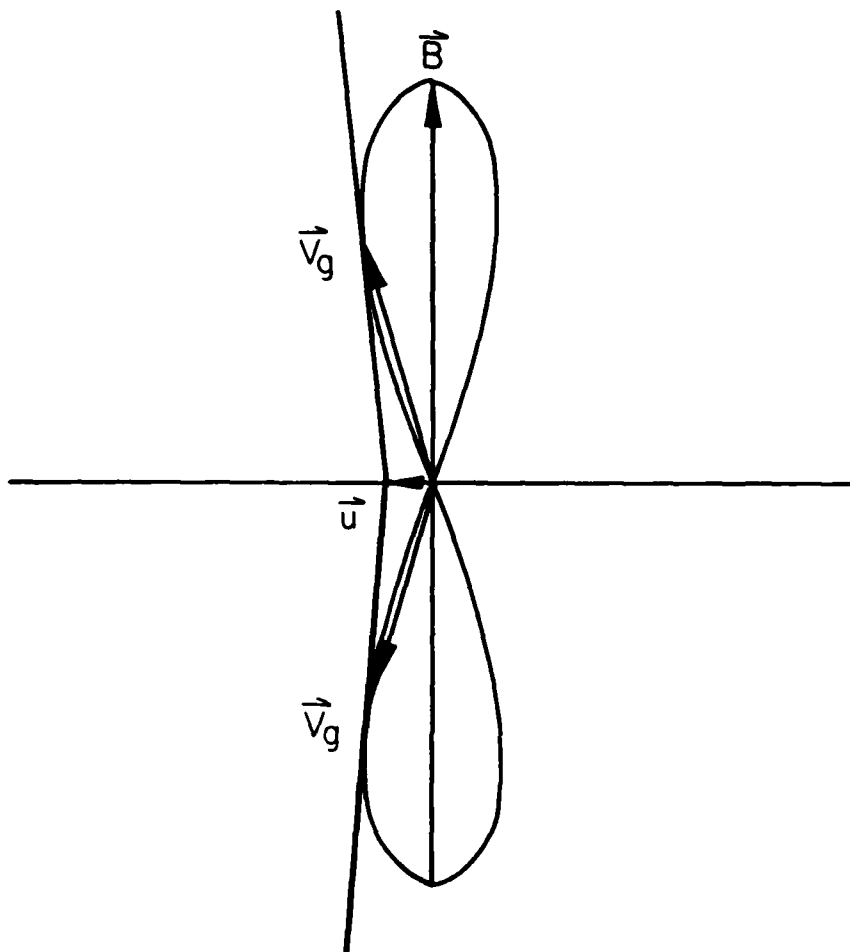


Figure 4. Construction of the Characteristics for a Moving Source. The polar plot is the group velocity locus; the magnetic field direction is indicated by the arrow. The source velocity is indicated by \vec{U}

determine all of the shock-like disturbances. It should be emphasized, however, that larger source velocities would introduce qualitatively new characteristic surfaces and the associated shock-like disturbances; an example is the fast mode Cherenkov cone.

In the limit of small spacecraft velocity, it is easy to see the qualitative nature of the changes in the characteristic surfaces and to discuss the nature of the

spacecraft interaction associated with them. Let us discuss the qualitative nature of the changes for two cases: $\epsilon_* < 0$ (Case 1) and $\epsilon_* > 0$ (Case 2).

Case 1: If the spacecraft velocity is across the field, shock-like disturbances can occur. Ahead of the spacecraft, the changes will be small. There will still be a well defined characteristic surface past which disturbances of a given frequency cannot spread. The angle this surface makes with the magnetic field will still be given to high accuracy by Eq. (44). Behind the spacecraft, the changes are more significant. Because the waves with zero group velocity in the proper frame do not propagate through the plasma, once they are produced, they will form a trailing wake behind the spacecraft. This is simply a statement of the fact that there is no characteristic surface in the spacecraft wake; unlike the case of a stationary source, there are no solutions in the wake of Eq. (133) for \hat{n} , as can be seen from Figure 4. Even though there are no trailing characteristics, the solutions obtained [Eqs. (92) through (100)] should still be reasonably accurate, except that the trailing disturbance will approach zero rapidly but not vanish.

If the spacecraft velocity lies within the characteristics, no shock-like disturbances are possible. For example, if the velocity is parallel to the field, the disturbance propagates (in the spacecraft frame) ahead of the spacecraft at several hundred kilometers per second and behind the spacecraft at the orbital velocity (several kilometers per second).

While the formal results have been obtained in two dimensions, we may apply them in a qualitative fashion to three dimensions. The application follows easily from the axisymmetric nature of the actual waves around the field in the proper frame. There is a two-lobed disturbance field. The dividing line between the two lobes trails the spacecraft antiparallel to the spacecraft velocity. The leading edge of the disturbance (ahead of the spacecraft) is a cone whose angle with respect to the field is given approximately by Eq. (44). Toward the sides of the cone, the disturbance is still sharply defined, with much the same cone angle. However, the trailing disturbance extends to infinity, growing narrower at large distances. A qualitative representation is shown in Figure 5. For the conditions of Figure 1, this configuration applies to Alfvén and whistler disturbances.

Case 2: If the spacecraft velocity is along the field, shock-like disturbances can occur. Inside the characteristics ahead of the spacecraft, there will be no disturbance. The main disturbance itself consists of two lobes, associated with the group velocity, directed across the field. Again, there will be a trailing wake. If the velocity lies outside the characteristics, then there are no shock-like disturbances.

In three dimensions, the disturbance is obtained by rotating the two-dimensional result around the field. The result is a conical leading disturbance with a trailing wave field. The main disturbance is expected to lie between two mirror

symmetry cones (for the case that \hat{U} is parallel to \hat{B}) with a smaller amplitude disturbance extending to infinity in the wake. A qualitative representation is shown in Figure 6. For the conditions of Figure 1, this configuration applies to upper hybrid disturbances.

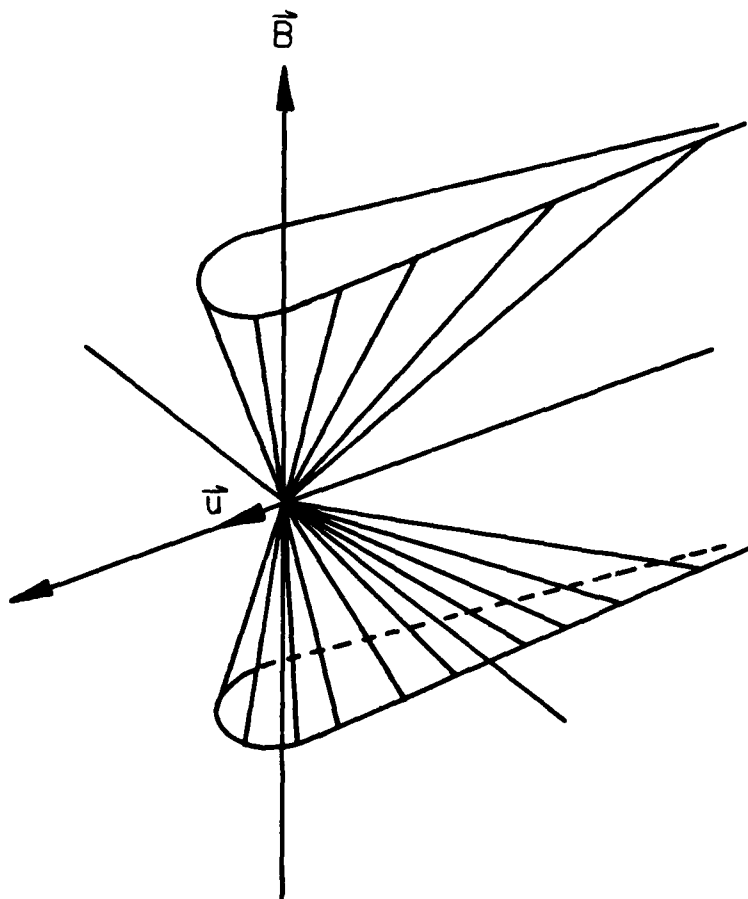


Figure 5. Qualitative View of the Three-Dimensional Limits of the Wave Field for a Given Frequency and $\epsilon^* < 0$. For the plasma of Figure 1, this behavior is typical of the Alfvén and whistler regions

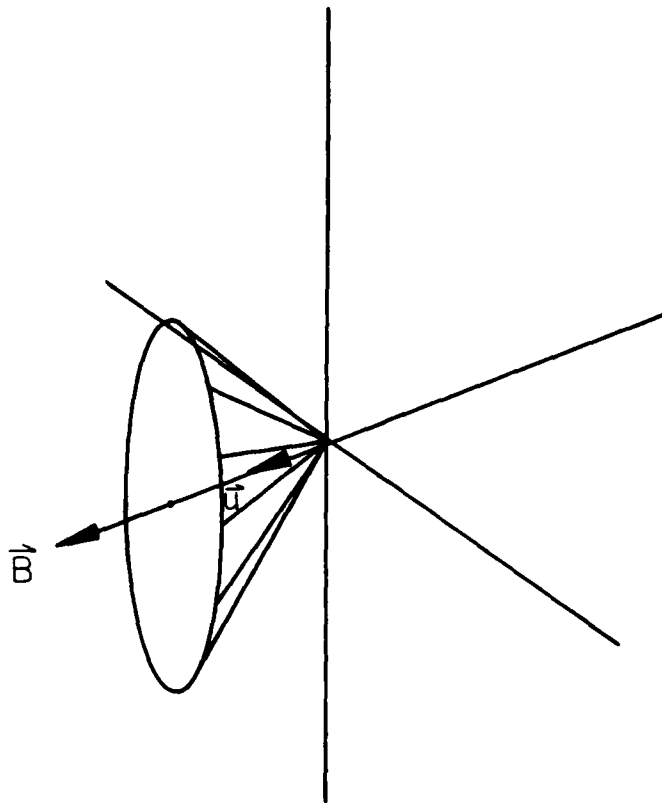


Figure 6. Qualitative View of the Three-Dimensional Limits of the Wave Field for a Given Frequency and $\epsilon_* > 0$. For the plasma of Figure 1, this behavior is typical of the upper hybrid region

7. DISCUSSION

We have investigated the properties of waves that are assumed to be produced as the result of the interaction of a spacecraft with a cold plasma. We have found that there are three distinct frequency regimes for which the waves can propagate to large distances from the spacecraft and cause shock-like disturbances. These waves may be roughly classified as Alfvén waves, whistlers, and upper hybrid waves. In the examples given in the paper, the Alfvén and whistler waves are guided along the geomagnetic field, while the upper hybrid waves propagate across the field.

The question of the production of these waves has not been dealt with. For the

purposes of this work, we have simply assumed the existence of a wave source and have treated the subsequent evolution of the waves. The production of Alfvén wings is reasonably well understood. They result from the steady charge separation required to maintain zero electric field, as seen by a comoving observer, inside a conductor moving across a magnetic field. The resulting electric field at the surface of the conductor then propagates along the Alfvén characteristics, forming steady Alfvén wings.

The production of higher frequency waves is not so easy to understand in any detail. In general, the wave spectrum associated with the spacecraft interaction should extend up to a frequency

$$\omega \approx U/L \quad (136)$$

where L is a typical dimension of the spacecraft. For a spacecraft about 10 m across, the maximum frequency is about 10^5 sec^{-1} . If smaller scale structures, such as wing tips and bay door edges (or, in general any structure with a small radius of curvature), are considered, then the maximum frequency is raised perhaps two orders of magnitude. So it appears that wave frequencies as high as the whistler and upper hybrid regions are possible.

On the other hand, the formal result for cold plasmas is that the spacecraft interaction produces only zero frequency waves as observed in the frame in which the spacecraft is at rest, as mentioned in the discussion following Eq. (123). While there are contributions to the steady structure from waves of all frequencies [see Eq. (123)], it is not at all clear that waves will be produced that oscillate in the spacecraft frame.

This makes clear an underlying assumption of the paper: While the propagation of cold plasma waves has been treated in some detail, we rely on processes outside of cold plasma physics to actually produce the waves. While little is known theoretically about such wave production, there are two lines of attack. One is to measure the wave field near the spacecraft. Given a measured source, the present formalism describes the subsequent evolution of the waves. The other is to generate a self-consistent model of the steady state Shuttle environment and analyze it for dominant plasma instabilities and again compute the evolution. Both types of effort are in early stages of development.

References

1. Stix, T.H. (1962) The Theory of Plasma Waves, McGraw-Hill, New York.
2. Musielak, Z.E. (1984) M.I.T. Center for Space Research Report No. CSR-TR-84-3.
3. Drell, S.D., Foley, H.M., and Ruderman, M.A. (1965) Drag and propulsion of large satellites in the ionosphere: An Alfvén propulsion engine in space, J. Geophys. Res. 70:3131.
4. Barnett, A., and Olbert, S. (1985) Radiation of plasma waves by a conducting body moving through a magnetized plasma, submitted to J. Geophys. Res.
5. Courant, R., and Hilbert, D. (1962) Methods of Mathematical Physics (Vol. II), Interscience, New York.
6. Jeffrey, A., and Taniuti, T. (1964) Non-Linear Wave Propagation, Academic Press, New York.

Appendix

The source terms for the wave equations can be introduced in the usual way. The Ampere-Faraday Law is

$$\vec{\nabla} \times (\vec{\nabla} \times \delta \vec{E}) = \epsilon_{ij} \delta E_j + (4\pi i \omega / c^2) \vec{J} \quad (A1)$$

where \vec{J} is the source current. The equations for the field fluctuations are

$$[\partial_z^2 + (\epsilon_P / \epsilon_0) \partial_x^2 - \epsilon_P] \delta B_y = \epsilon_H \delta B_x - (4\pi / c) [\partial_z J_x + (\epsilon_P / \epsilon_0) \partial_x J_z] \quad (A2)$$

$$(\partial_x^2 + \partial_z^2 - \epsilon_P) \delta B_x = -\epsilon_H (1 + \epsilon_0^{-1} \partial_x^2) \delta B_y + (4\pi / c) \partial_z J_y \quad (A3)$$

The equations for the amplitudes α and β are

$$[\partial_z^2 - (\epsilon_0 / \epsilon_P) \partial_x^2 - \epsilon_P] \alpha = \epsilon_H (1 + \epsilon_0^{-1} \partial_x^2) \beta + (4\pi / c) [-(1 - \epsilon_0 / \epsilon_P) \partial_z J_x - (\epsilon_H / \epsilon_0) \partial_z J_y - (1 - \epsilon_P / \epsilon_0) (\epsilon_P / \epsilon_0) \partial_x J_z] \quad (A4)$$

$$(\partial_z^2 + \partial_x^2 - \epsilon_P) \beta = -\epsilon_H \alpha + (4\pi / c) [-(\epsilon_H / \epsilon_0) \partial_z J_x - (1 - \epsilon_P / \epsilon_0) \partial_z J_y - (\epsilon_P \epsilon_H / \epsilon_0^2) \partial_x J_z] \quad (A5)$$

In the text, the right-hand sides were treated as delta functions. A proper physical treatment requires that the current density be the delta function source. The qualitative result is that the expressions in the text must be differentiated with respect to the appropriate variable (for example, z if the source term is $\partial_z J_x$) and then multiplied by the appropriate coefficient [for example, $-(4\pi/c)(1/\epsilon_0/\epsilon_P)$ for the leading term in Eq. (A4)].

END
FILMED

5-86

DTIC